

Research article

VADOCHARGE: Groundwater Recharge Model for an Uplifted Island Karst Aquifer, Guam, USA

Nathan C. Habana^{1,2}, Leroy F. Heitz¹, Arne E. Olsen¹, John W. Jenson¹,
Jonathan L. Salvacion²

¹Water Environmental Research Institute of the Western Pacific,
University of Guam, Mangilao, Guam, Guam USA
nhabana@uguam.uog.edu, lheitz@uguam.uog.edu, jjenson@uguam.uog.edu
+1-671-735-2685 fax: +1-671-734-8890

²Mapúa Institute of Technology, Graduate Studies, Intramuros, Manila, Philippines
jlsalvacion@mapua.edu.ph
+63-2-527-3681

ABSTRACT

The Northern Guam Lens Aquifer (NGLA) presents unique challenges to modelers due to the complex hydrologic properties of its thick karst vadose zone. To meet these challenges, we developed VADOCHARGE, an analogue model based on the US Army Corps of Engineers' Streamflow Synthesis and Reservoir Regulation (SSARR) model, to produce the effect of attenuated and lagged recharge through the vadose zone to the water table. It incorporates a soil moisture model to account for soil moisture storage, evapotranspiration, and recharge determined by a soil moisture curve relationship. To simulate flow through limestone bedrock, the model applies time storage routing technique in a series of reservoirs, to simulate the time arrival of both fast and slow recharge past the soil to the water table reach. The model is implemented by assigning recharge from the portions of the surface watershed to each node of an underlying coupled phreatic model. Several simulations were performed and adjustments to hydraulic parameters were made until a close match with observation well data was achieved. The results improved upon all former models of the NGLA, and provide the tool for sophisticated and accurate coupled vadose-phreatic models of the NGLA and similar karst aquifers. **Copyright © IJESTR, all rights reserved.**

Keywords: deep karst vadose aquifer recharge model, evapotranspiration, analogue hydrologic routing

1. INTRODUCTION

Uplifted carbonate islands, such as Guam (Figure 1), presents special challenges to groundwater modelers [cf., 7, 18]. On Guam's Northern Guam Lens Aquifer (NGLA), meteoric recharge must transit 60 to 180 m of vadose limestone bedrock to reach the water table, near sea level (Figure 2), which percolating and streaming flows may reach the water table in lagged and attenuated fashion. In this vadose zone, the spatial variations of hydrogeologic parameters are typical of karst aquifers which are quite difficult to accurately quantify. Such physical complexity of karstic aquifers makes Darcian model parameters difficult to assign, requiring much adjustment to match field observation well levels. Moreover, surface infiltration is not only controlled by soil and vegetation conditions, but

seasonal soil moisture and rainfall intensity also control the relative distribution of surface infiltration between slow, diffuse percolation through the bedrock matrix on the one hand, and vadose fast flow by direct routes that bypass the percolating water. On the other hand, previous studies suggest that percolation can take up to 20 months or more, while fast flow may deliver substantial amounts of meteoric water to the water table in only a few hours, maybe even minutes [21].

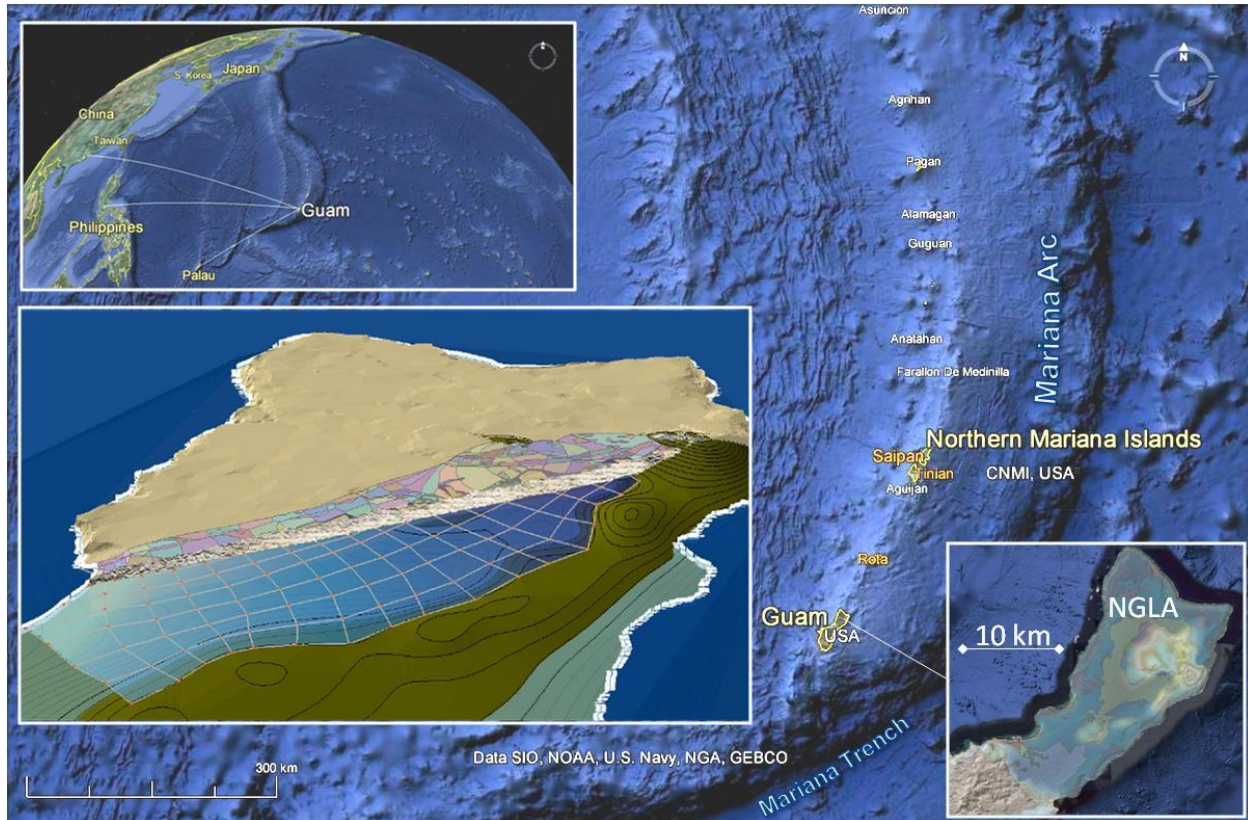


Figure 1. Slice through NGLA Yigo-Tumon Trough groundwater sub-basin, study domain. The NGLA is an uplifted island karst aquifer, having high permeability, resting on a low permeable volcanic basement (see Figure 3). The finite element mesh is fixed at mean sea level in the phreatic zone. Map source: Google Earth™.

The difficulties of accommodating both the complexity of surface conditions and vadose processes into coupled numerical models of vadose and phreatic groundwater flow have motivated development of a novel approach to vadose modeling of this karst aquifer, embodied in a new analytical model, VADOCHARGE, which we present in this paper. VADOCHARGE introduces the idea of modeling the passage of meteoric recharge through the unsaturated zone as a soil moisture budget and its transfer by an imaginary series of phase cells through the thick limestone bedrock, and then shows how this basic concept can be adapted to simulate the co-existing fast and slow bulk flow rates that are found in deep uplifted karstic aquifers. The approach has potentially wide application, as it links the simple accounting models normally used to determine recharge with groundwater models that are in turn significantly influenced by that recharge.

The model structure is best suited to simulating bulk flow through the vadose zone. However, it does not represent the actual structure of the unsaturated aquifer realistically. The successive cells or reservoir phase cells of the flow routing model represent depth increments in the aquifer. At each cell in a vertically aligned series, the lumped reservoirs are not equivalent to flow through a finite thickness of porous medium. The equivalent behavior of the model simulation to the real world rests on the fact that both introduce time delays and have storage dependent outflows. The choice for using watershed streamflow methods was realized through the similarity of observation well data to that of surface hydrology [8, 13]. The general applicability is that attenuated and lagged recharge, rather than instantaneous, is achievable through this modeling approach. Also, in the SSARR watershed model,

routing does not focus on the physical detailed complexity of water paths in a watershed, but rather on the simulation of time distribution of flow rate response matched to a stream gage, from rainfall input, in the shape of a hydrograph. The SSARR model applies surface flow as fast flow routes, which may be analogous to fast transfer of moisture through conduits and fractures in unsaturated karsts; while the SSARR subsurface flow is much slower, which is like the percolation flow through matrix pores in the vadose zone. Furthermore, rather than a delineated watershed as in surface hydrology, this model catchment area is fixed upon every finite element mesh node cells of an underlying phreatic model finite element mesh, depicted as vertical geologic shafts extending from the water table to the surface. These fixed model unit network can be thought of as node watersheds, termed here node-sheds.

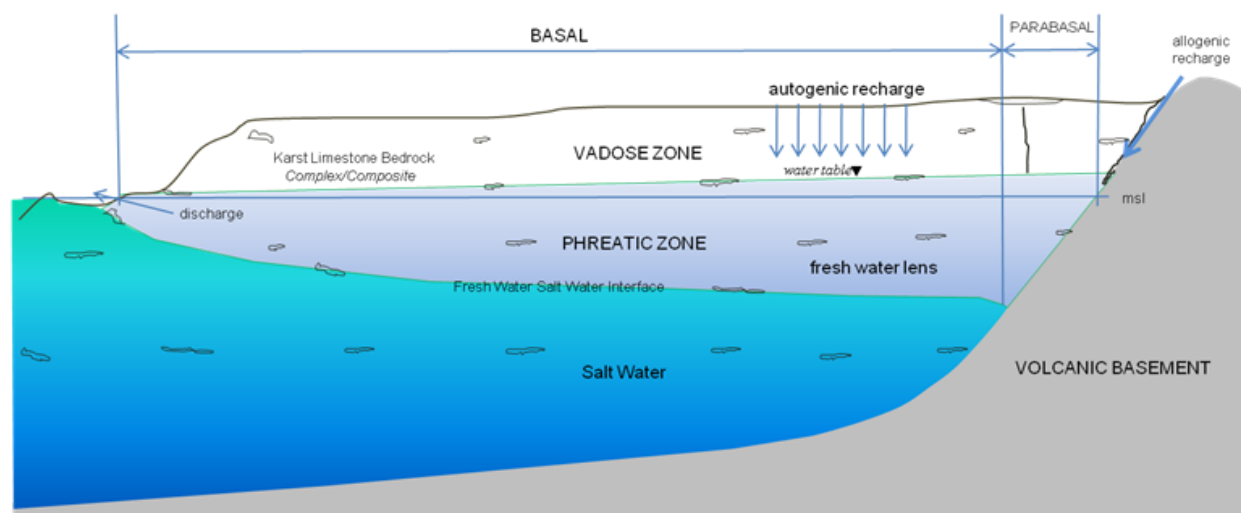


Figure 2. Schematics of the NGLA. An unconfined fresh water lens aquifer that receives autogenic and allogenic recharge. The aquifer's thick vadose zone and triple porosity affect the time arrival of meteoric recharge.

2. AQUIFER CHARACTERISTICS

The development of VADOCHARGE is based on a continuously progressive understanding of the aquifer characteristics in which the conceptual model is conceived, including field data and observations of the physical media and its hydrologic cycle. Recharge is defined here as the meteoric moisture that reaches the water table and not necessarily the effective recharge that is stored in long periods in the phreatic zone that forms the lens.

2.1. Hydrology and Hydrogeology

Guam's climate is tropical wet-dry, with an annual average rainfall of approximately 2500 mm. About 30% arrives during the dry season, usually January through June, and 70% during the wet season, usually July through December. August and September are the peak months, for which the record high is 970 mm in August 1997. March and April are the driest, with March having roughly 70 mm of rainfall [28]. El Nino events bring low sea levels up to December, but also increased risk of strong tropical storms; conversely, La Nina events bring high sea levels, but reduced risk of tropical storms [20].

The NGLA is composed primarily of the Miocene-Pliocene *Barrigada Limestone*, which forms the core of the aquifer and grades upward and outward into Pliocene-Pleistocene *Mariana Limestone* [30]. The *Barrigada Limestone* is a detrital, mostly foraminiferal bank deposit. The *Mariana Limestone* comprises the overlying lagoonal and surrounding reef deposits built on and around the Barrigada deposit as it rose into the photic zone. The surface of the aquifer is a faulted and tilted karst plateau standing 60-180 m above modern sea level. The basement beneath the limestone bedrock aquifer is an Oligocene mostly volcanoclastic unit with complex subterranean topography [30, 40, 23, 38] and its hydraulic conductivity is several orders of magnitude smaller than the limestone. Topographical ridges in the basement above sea level thus partition the phreatic zone of the aquifer into six sub-basins (Figure 3) and shunt descending vadose waters down the flanks of the basement ridges to the recharge boundary of the water table, as allogenic recharge. The map shows a semi-transparent relief map for visualizing through the limestone overlay. Beneath the limestone is the volcanic basement and where it rises above the water table provides the barrier that divides the NGLA into 6 management sub-basins: Finegayan, Agafa Gumas,

Andersen, Yigo-Tumon, Mangilao, and Hagåtña. The study area is situated in the Yigo-Tumon Basin. At Mount Santa Rosa and Mataguac Hill, which occupy only about 2% of the plateau, the volcanic basement crops out above the plateau. Surface runoffs from the flanks of these features are carried by ephemeral streams into insurgences in sinkholes that occupy the flanks of the outcrops.

The current vadose section has been generally emergent throughout the Pleistocene. The modern phreatic section has spent a substantial amount of the Pleistocene as vadose rock, with exposure time increasing upward from the depth of the lowest of the relative Pleistocene sea level depressions (perhaps some 130 m). Lens has migrated up and down this thick aquifer as sea levels have changed, thus has historic important implications for the distribution of hydraulic conductivity throughout the aquifer. In particular, the current model of carbonate island karst [17] predicts that mixing and flow of phreatic water near the water tables and saltwater interfaces of ancient freshwater lens produced laterally extensive zones with enhanced hydraulic conductivity [35].

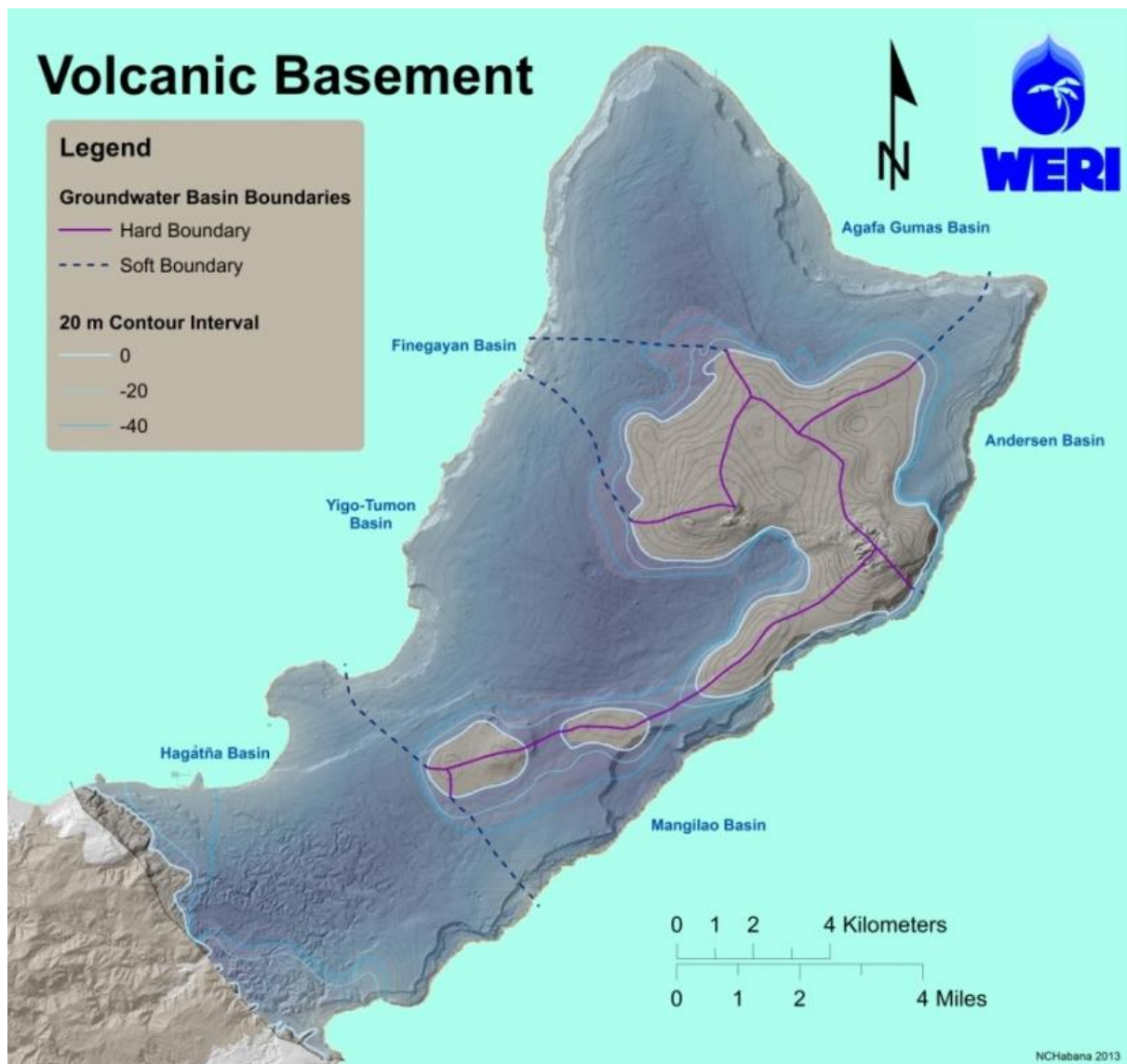


Figure 3. The 6 subsurface basins of the NGLA. Data Sources: WERI [38], Guam Bureau of Statistics and Plans.

The matrix porosity is generally composed of weakly cemented granular or spongiform limestone that is still permeable enough for water to make its way around small rock particles and through tiny, even microscopic, connective pores. Vadose dissolution along limestone-volcanic contacts is known to have produced significant contact caves that deliver vadose water in stream flow to the water table boundary [cf., 24]. Regionally extensive

fractures, enlarged by dissolution, have been known to carry storm water several kilometers in only a few days [24, 15] and probably help account for the extremely high regional conductivity, which previous modeling and field studies [17] have estimated to be about 6,000 m/day. Pump tests in the Barrigada Limestone produced local hydraulic conductivities up to 150 m/day [5]. The NGLA is thus a triple-porosity aquifer [41], in which storage, transport, and discharge are governed by the interaction of substantial residual primary porosity in the limestone matrix as well as locally and regionally important fracture flow, and regionally significant conduit flow.

2.2. Soils and Surface Infiltration

In the domain at the plateau surface, 23% is urban land complex, having no significant soil cover. The greatest soil area coverage, 65%, is Guam cobbly clay loam. Where present, soils are relatively thin, with average thickness of about 25 cm and field capacities range from 10 to 100 mm [34]. Areas without soil are very permeable, and where undeveloped, ponding is never observed. Arguably, the most significant contribution of the soil cover is that when wet it supports overland flow, shunting surface runoff to closed karst depressions from which it can descend rapidly to the water table. Areas with no civil development, with or without soil cover, are typically overgrown by limestone forest of dense, shrubby secondary growth. The vegetation covers more than 65% of the surface, but the 60 to 180 m elevation of the plateau precludes any vegetation from extending roots to the water table.

Jocson et al. [18] noted that some 22% of annual rainfall arrives in intermittent showers on days receiving 6 mm or less. Under such conditions, especially during the dry season, it seems likely that much of such rainfall evaporates directly from canopy storage or the ground surface, and that little of whatever remains makes it past the root zone. At the other extreme, some 20% of the total rainfall arrives on days receiving 5 mm or more, mostly during the wet season. Under these conditions, the soil layer is generally at or near saturation, favoring surface runoff to local closed depressions, of which many in developed areas have been deepened into ponding basins to enhance storage, and some have even had injection wells installed to enhance infiltration. A large portion of the heaviest rainfall is thus thought to descend through the vadose zone via fast flow routes. Recharge to the lens thus arrives by various routes in different quantities at different times because it travels the vadose zone's great depth through different pathways—connective pores, fractures, shafts, and caves—to get to the lens.

Surface streams do not form on the plateau, except on the flanks of Mount Santa Rosa and Mataguac Hill in the northeastern part of the plateau and the Hagatna Sub-basin at the southern end of the plateau. On the Santa Rosa and Mataguac rises, ephemeral streams that form during heavy rains deliver storm water to swallow holes in sinkholes formed at the contact of the volcanic basement outcrops and the surrounding limestone bedrock. In the Hagatna Sub-basin, the surface limestone is mapped as the Argillaceous Member of the Mariana Limestone. It received siliciclastic input from streams draining from the adjacent volcanic uplands into the Mariana lagoon, and may be extensively underlain by the clean, harder, strongly re-crystallized Alifan Limestone, a Miocene reef deposit, which is exposed in fensters near the southern part of the sub-basin [30]. The Hagatna Sub-basin is unique in the NGLA in that it possesses surface streams, including some permanent streams that drain to the coast, as well as classic karst features including ephemeral streams that disappear in classic blind valleys. Pump tests of wells [5] in this basin exhibit local hydraulic conductivity of only 10 to 25% (i.e., up to 50 m/day) of the best fit regional hydraulic conductivity 6,100 m/day [18, 6, 7]. In the context of other karst aquifers [cf., 1, 9] estimates of 90 m/day for karstic fissured aquifers, the NGLA hydraulic conductivity is very high by comparison. Ayers and Clayshulte [3] and Rotzoll et al. [26] applied the Jacob-Ferris model for the NGLA, using tide signals, resulting hydraulic conductivities ranging from 1,200 - 6,300 m/day.

2.3. Previous Related Research

The first documented attempts to estimate aquifer recharge date back to the work of Stearns [29]. Other efforts up to the 1970s were reported by Ayers [2] using various techniques including water budget of southern Guam to derive and estimate of recharge for northern Guam. In a Northern Guam Lens Study [5] and Sustainable Yield and Ground Water Development [23], Mink's "most-probable" estimate was 60-65% of annual rainfall goes into recharge. Improved data availability in several methods produced daily estimates of approximately 3400-3800 m³/km² [18, 12].

As part of the Northern Guam Lens Study, Contractor [6] developed a 2-dimensional finite-element model of phreatic flow. In this and subsequent, improved models [7] minimum recharge was estimated for monthly time-steps by subtracting total monthly pan evaporation from total monthly rainfall, and assuming that the difference was delivered to the water table within the same month. Jocson et al. [18] refined the recharge estimate by calculating daily minimum recharge from daily precipitation minus daily pan evaporation, but summed the daily estimates into

monthly totals and applied the same assumption that monthly recharge thus estimated reached the water table within the same month. The authors of each of these modeling studies noted, however, that comparison of simulated water table response with actual water table response indicated that a substantial portion of the flow captured each month must be delivered to the base of the vadose zone over longer spans of time. These early studies however had no means of estimating the proportion or timing of water delivered by fast flow routes.

Contractor and Jenson [8] applied a 1-dimensional vadose model based on Van Genuchten and Nielsen [36] to distribute over time to each node in the phreatic model. They also incorporated a “bypass” route [cf., 10, 27] to accommodate vadose fast flow, noted that the best fit between simulated and observed water table response was obtained when 32% of the monthly recharge was assigned to fast flow. In spite of the improved results, however, this approach required running the 1-dimensional vadose model at daily time steps and numerous nodes at each of the several thousand nodes in the phreatic model, which increased the computer run time by between one and two orders of magnitude.

3. METHODS - MODEL DEVELOPMENT

The development of VADOCHARGE required detailed examination of data and field observation as interpretations of the real system, as discussed previously. In the methods, model development is explained progressively in standard process of model development [cf., 14, 4]; conceptual model, mathematical model, numerical model, and computer model.

3.1. Conceptual Model

The triple porosity of the aquifer is impossible to capture in fine resolution, so models must assume representative composite properties. Although the phreatic zone has been successfully modeled at the regional scale using Darcian models with hydraulic conductivity of 6,000 m/day and porosity of 0.2 to 0.25 [cf., 17], modeling the vadose zone presents special challenges, as described above. The conceptual model described below thus includes a soil moisture model, and transfer model. The transfer model is a variation of *modified puls* routing technique, also referred to as SSARR time of storage routing [32, 33] that assign appropriate portions of infiltrating recharge to either slow percolation or fast flow and determine the arrival times of each. This section describes the conceptual model and its relationship to analytical components of the model. The subsequent section, describes the analytical components and their implementation.

3.1.1. Watershed Hydrogeography

The model domain is situated in the Yigo-Tumon basin of the NGLA (Figure 3) for the area of study. This area was preferred since it had the best continuous available monitoring data, M-10a and M-11, (USGS observation wells, Figure 4) and is an economically significant source. Figure 4 is a finite element mesh, showing the nodes over which the vadose node-sheds are centered and the boundary conditions of the coupled model. In this domain are two USGS observation wells (red markers) M-10a and M-11. The nodes are assigned phreatic model influx conditions.

To implement the model, the spatially varied surface data is developed upon the base phreatic model (Figure 4). The domain finite element mesh is first sectioned into node cells [37], virtually extruded to the surface as a vadose shaft, termed “node-shed,” defined as a surface and vadose hydrologic node watershed (Figure 5), done with Euclidean allocation (GIS Spatial Analyst tool), similar to Theissen polygons in hydrology. Each node-shed contains the sub-polygon zones bounded with light grey lines. Boundary flux node-sheds were edited to extend to the basement volcanic ridge to include the area contributing to allogenic recharge. Nodes 41 and 59 are positioned on observation wells M-10a and M-11 respectively. These node-sheds are centered directly above the nodes of underlying phreatic domain, aligned directly above a node and of the same area as its respective node-cell, of which contains GIS layers of the relevant hydrological data (rainfall, pan evaporation, soil, zone properties and node-shed properties) from which recharge for the phreatic node is ultimately calculated. The node-shed receives the daily rainfall input and contains unique sub-polygons (zones) (Figure 6) to which are assigned the attributes for the soil moisture model that determine the proportions of rainfall that go to recharge, evapotranspiration, and remaining soil moisture. The evapotranspiration effect proportions are determined for each node-shed by an adjustable soil moisture properties curve [39], which provides the percent yields to evapotranspiration. The moisture to recharge is excess to the threshold of a soil’s field capacity, which when less than field capacity remains in soil moisture held by soil and moisture adhesion and excess is gravitationally percolated.

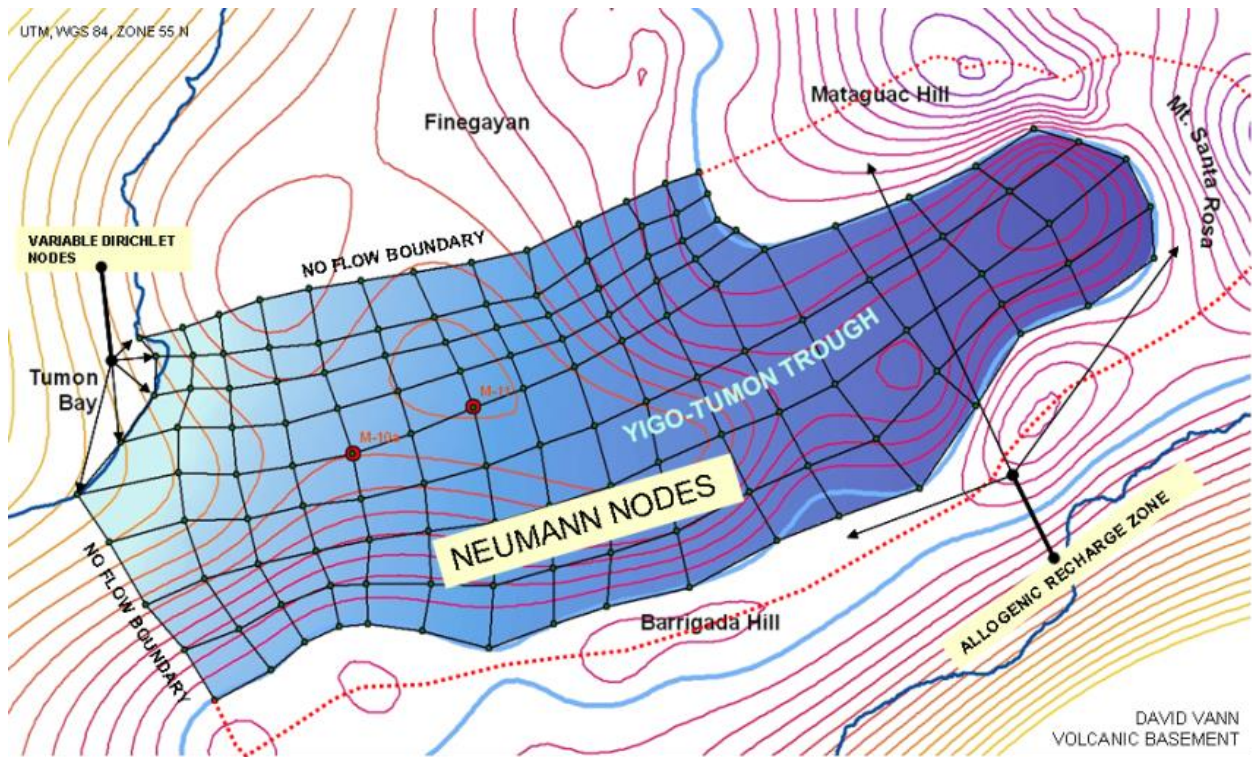


Figure 4. Domain of the underlying phreatic model.

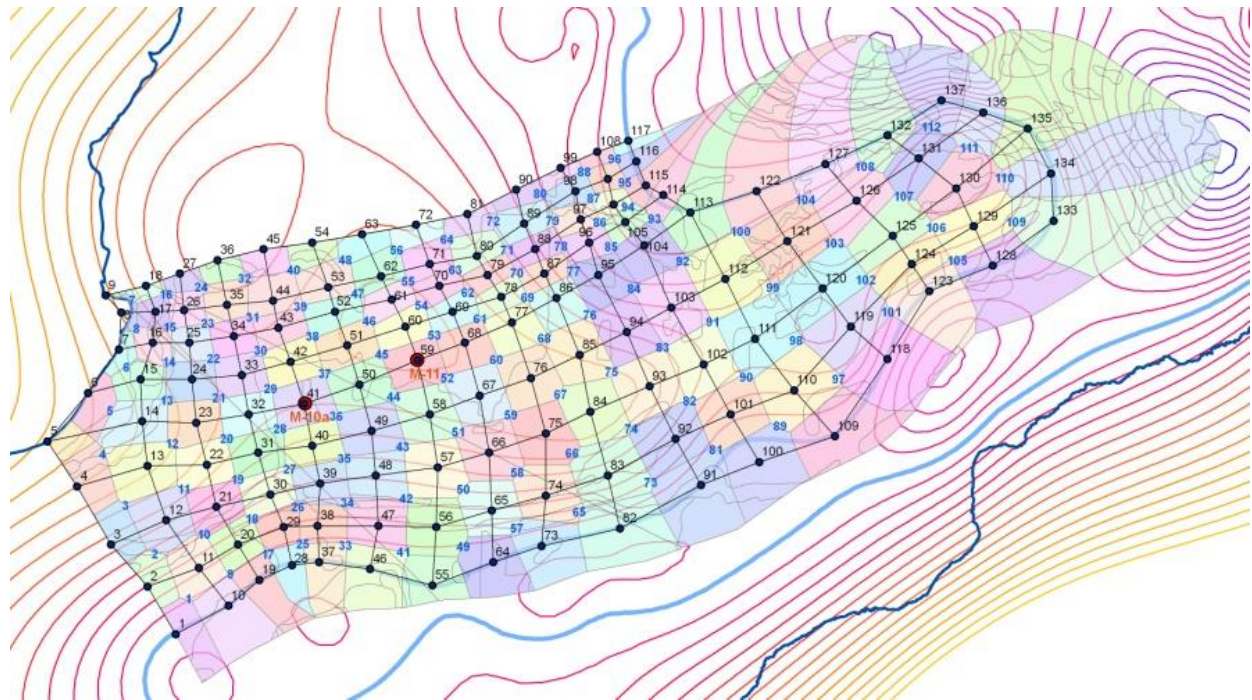


Figure 5. GIS compilation of the domain showing watershed domain node-sheds overlying the finite element mesh nodes of the underlying phreatic domain.

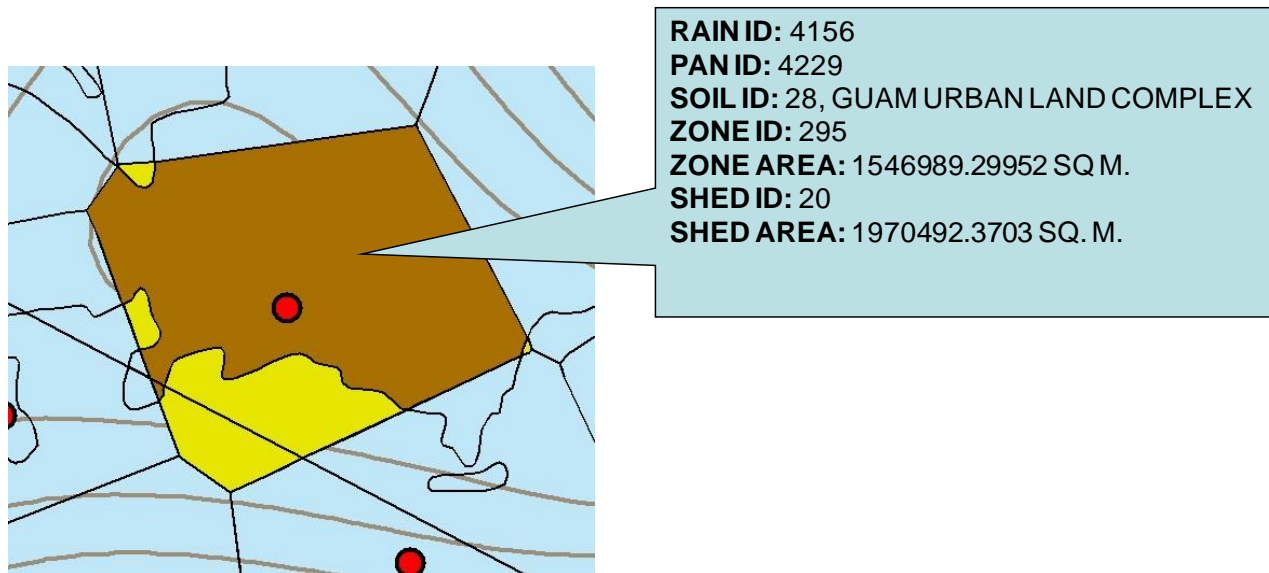


Figure 6. Node-shed for node number 20, containing sub-polygons called zones. The zones have unique attributes.

3.1.2 Node-shed Conceptual Model

The vadose column of bedrock is treated as a vertical stream. Percolation (slow flow) through the matrix of small interconnected pores, which supply water to fractures and conduits in the bedrock aquifer, is modeled like subsurface flow to a stream in a watershed model. Fast flow (through fractures and conduits) is modeled like direct surface runoff to a stream in a watershed model. A routing routine, described in the next section, is used for simulating the travel time and storage in the vadose zone.

Allocation of infiltrating water between fast and slow flow is controlled by bedrock fast-slow moisture split curve. This split curve is also used in the SSARR model [31], to fractionate moisture input that will move into surface flow as runoff into a stream, and the remaining moisture into subsurface flow, which applies to the analogy of fast and slow flows discussed previously. The SSARR model is detailed however, considering several curves for discrete intensities of rainfall and the curves are empirical, while VADOCHARGE applies the same concept but is adjusted during calibration to observation well data. Observation well and rainfall analysis also reveal that it takes a certain amount of rainfall for the aquifer to show a significantly sharp response, which is an S curve relationship. The split curve has input moisture is in the x-axis and the y-axis is percent split to fast by the assigned curve, the other portion moves moisture into slow flow. A cascading reservoir routing routine is used to calculate time of storage and phases for the fast and slow components. The time of storage produces the effect of attenuation while the number of phases determines time delays or lag between the rainfall events and its arrival to the water table.

In Figure 7, the first stage depicts the soil moisture model and the area-weighted average (AWA) recharge component. The model solves for the soil moisture split between recharge and evapotranspiration using a soil moisture model equation for each zone in a node-shed throughout the entire domain on a daily time step. The area-weighted average for the node-shed's varying recharge in each zone is depicted as the bottom dark blue layer. The second stage is the modified pulse-routing component. The two glass tubes represent the modified pulse routing system. The large and thin glass tubes handle the fast flow and slow flow respectively. The bulbs represent the time in storage like an hour glass as vertical weirs, and the number of bulbs determines the delay. Each node-shed produces recharge for a specifically assigned node for the hydraulic model. The total volume of water delivered to the phreatic node is the sum of fast and slow recharge in a single time-step.

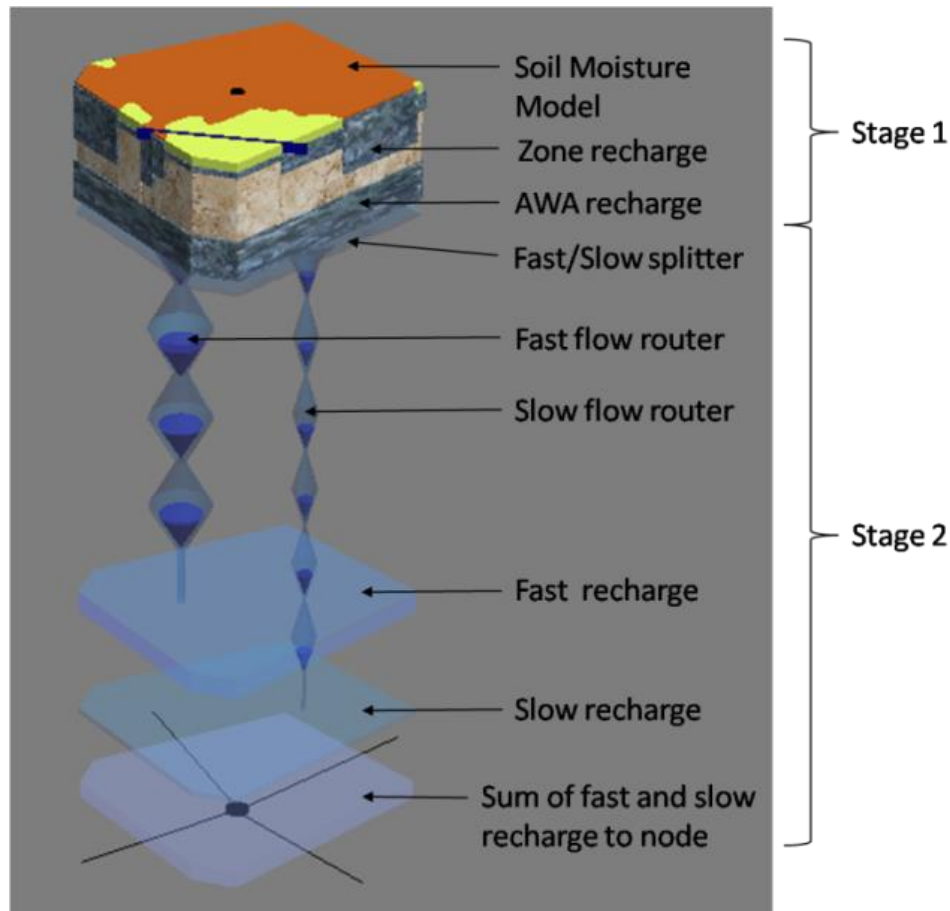


Figure 7. Node-shed conceptual model. The conceptual flow model connecting the vadose node-shed with the underlying phreatic node, showing the model's two-stage system.

3.2. VADOCHARGE Quantification

VADOCHARGE computations in both the soil model and the router apply hydrologic modeling which is based on the continuity equation (1), which maintains the conservation laws. The rate of change of moisture stored in a porous media confine is the difference of inflow and outflow rates.

$$\frac{dS}{dt} = I - O \quad (1)$$

Equation (1) is arranged into a numerical iterative solution to account for the soil system moisture exchange.

$$\frac{dS}{dt} = \lim_{t \rightarrow 0} \frac{\Delta S}{\Delta t} \Rightarrow \frac{dS}{dt} \cong \frac{\Delta S}{\Delta t} = \frac{S_2 - S_1}{t_2 - t_1} = \frac{S_2 - S_1}{\Delta t} \quad (2)$$

$$\frac{S_2 - S_1}{\Delta t} = I - O, \quad S_2 = S_1 + (I - O)\Delta t, \quad S_2 = S_1 + I_2 - O_2 \quad (3)$$

The time step is daily and the subscripts 1 and 2 refer to previous and current day period respectively. This equation is used to form the soil moisture model equation with consideration to soil field capacity, moisture to recharge, and evapotranspiration. The router is derived from the centered finite difference form [11] or average form of the continuity equation.

$$S_2 - S_1 = t(\bar{I} - \bar{O}) \quad (4)$$

$$S_2 - S_1 = t \left(\frac{I_1 + I_2}{2} - \frac{O_1 + O_2}{2} \right) = t \left(\bar{I} - \frac{O_1 + O_2}{2} \right) \quad (5)$$

Equations (3) and (5) are further refined to boundary conditions described in the following subsequent sections.

3.2.1. Soil Moisture Numerical Model

The soil moisture model is arranged for the current period soil moisture storage. Equation (3) storage variable is substituted by storage account of soil moisture, SM .

$$\begin{aligned} S_2 &= S_1 + I_2 - O_2 \\ SM_2 &= SM_1 + I_2 - O_2 \end{aligned} \quad (6)$$

Equations (7-9) are intermediate computation of soil moisture storage and recharge. A minor intermediate conditional variable, smi , is introduced to account for rainfall input, R , and previous period soil moisture.

$$SM_2 = \frac{SM_1 + I_2 - O_2}{smi}, \quad I_2 = R_2, \quad smi = SM_1 + R_2 \quad (7)$$

Soil moisture is limited by field capacity of the soil, FC , and smi is used in the condition (9) to compute the major intermediate soil moisture, SMI . The excess moisture that passes through the soil media as part of the output moisture that will move to recharge, RE , with respect to conditions.

$$SMI_2 = \begin{cases} FC & | smi > FC, \quad RE_2 = smi - FC \\ smi & | smi \leq FC, \quad RE_2 = 0 \end{cases} \quad (8)$$

The other part of the output moisture that leaves the soil media is by evapotranspiration, ET .

$$ET_2 = P_2 \cdot ETP_{(SMI_2/FC)} \quad (9)$$

ET is computed as the pan evaporation, P , multiplied by the evapotranspiration percent factor, ETP , which is dependent on the ratio of SMI and FC referred to as percent of field capacity. ETP is based on soil moisture and ET relationship models of Viemeyer, Pierce, and Thornthwaite [39]. Figure 8 shows the curve relationship for all three models. For soil moisture that is less than field capacity as percent of field capacity, there are several curve models to estimate evapotranspiration as percent of pan evaporation (considered potential evaporation). The percent may be determined by curve function or interpolation. The current period iteration soil moisture is thus computed daily.

$$SM_2 = SMI_2 - O_2, \quad O_2 = ET_2 \quad (10)$$

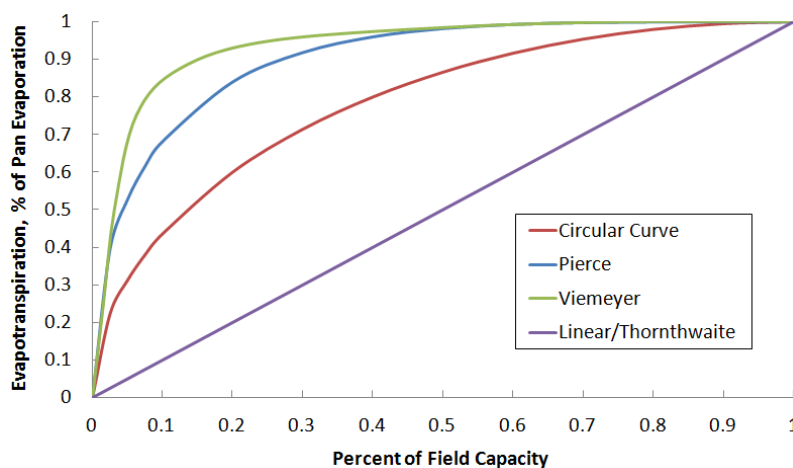


Figure 8. Evapotranspiration soil moisture relationship curve models. Modified from Source: Ward and Trimble 2004.

3.2.2. Moisture to Recharge

A node-shed may consist of surface feature sub polygons called zones, z , with unique attributes, producing varied recharge results for any node-shed. The model is made optional to compute the daily node-shed moisture to recharge as an area weighted average recharge (11) or the total moisture to recharge (12), where $RE_{ns,2}$ is the current node-shed recharge, $RE_{zi,2}$ is current recharge for a specific zone in a node-shed, and A_{zi} and A_{ns} are areas of zones in the node-shed and area of the node-shed respectively.

$$RE_{ns,2} = \sum_{zi}^{\text{zones in node-shed}} \frac{A_{zi}}{A_{ns}} RE_{zi,2} \quad (11)$$

$$RE_{ns,2} = \sum_{zi}^{\text{zones in node-shed}} RE_{zi,2} \quad (12)$$

The results of (11) or (12) is the bulk moisture past the soils of a node-shed and it is computed for every node-shed in the model domain in a daily cycle.

3.2.3. Moisture to Recharge Split and Routing

Moisture past the soil is modeled into two rates of fast and slow. The node-shed moisture to recharge computed by either (11) or (12) is split by percent curves similar to the evapotranspiration model. Figure 9 shows the SSARR and VADOCHARGE curve models that split the bulk flow to its respective router, fast or slow. Curve A is the SSARR split curve relationship to determine the portion of the watershed rain catchment that will proceed to the surface runoff router. Curve B is the split curve used in VADOCHARGE to determine percent of moisture to recharge in a node-shed that will transfer moisture to the fast router [31]. The remaining percent of moisture moves to the slower router. Field observation well data and rainfall data reveal the temporal response of groundwater levels depend on the increasing and intensified amount of moisture input. The percent may be determined by function or interpolation. A fast response is observed with more than 1 cm of rainfall. The SSARR model uses empirical intensity curve sets (e.g. 1 in/hr, 0.5 in/hr, etc.). VADOCHARGE in this phase of its model development use single curve that can be uniquely modified for each node-shed. The splitted moistures are then inputted into its respective fast and slow routers.

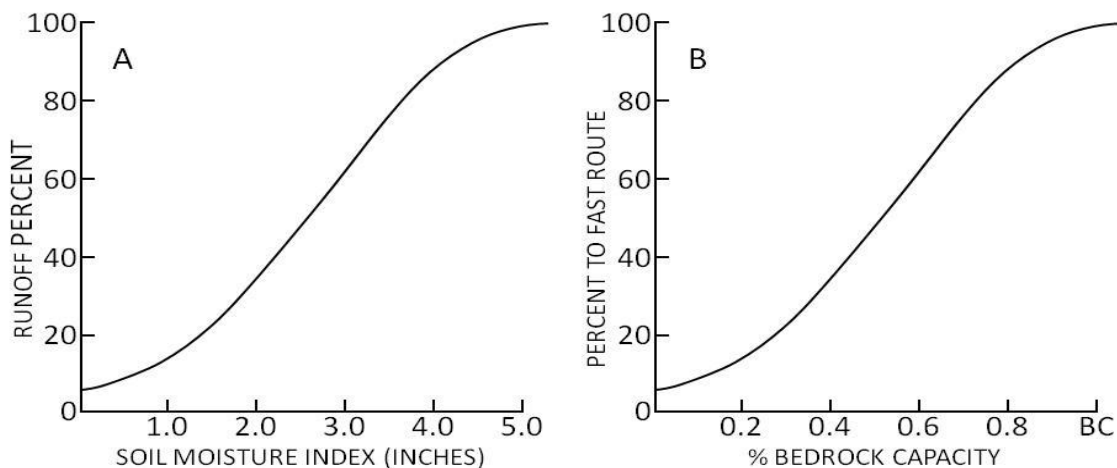


Figure 9. Moisture split curve concept.

The router is an effective algorithm for distributing input pulses over time periods, producing hydrographic simulations which may be the recharge fashion for thick karstic aquifer systems. The SSARR router is derived from the average or difference form of the continuity equation (5). The moisture storage, S , and unit outflow, O , periods form a linear relationship that defines time in storage, T_s (Figure 10).

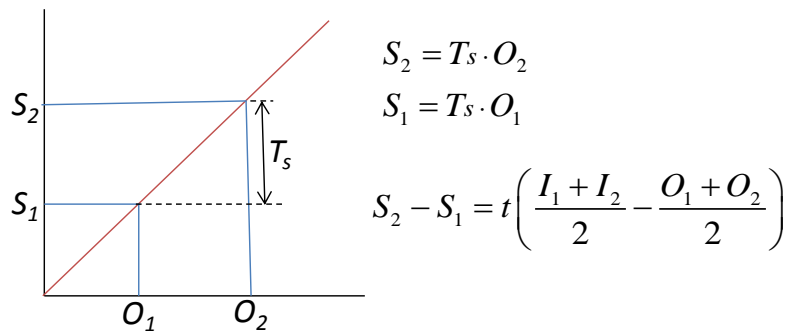


Figure 10. Time in Storage and linear relationship with storage and output periods.

Storage equations in the figure above are substituted into the main equation and expressed as (13) and further rearranged to solve for the current period output (14).

$$T_s \cdot O_2 - T_s \cdot O_1 = t \left(\bar{I} - \frac{O_1 + O_2}{2} \right) \quad (13)$$

$$T_s \cdot O_2 + \frac{t}{2} O_2 = \bar{I}t - \frac{t}{2} O_1 + T_s \cdot O_1$$

$$\left(T_s + \frac{t}{2} \right) O_2 = \bar{I}t - \frac{t}{2} O_1 + \left(\frac{t}{2} O_1 - \frac{t}{2} O_1 \right) + T_s \cdot O_1$$

$$\left(T_s + \frac{t}{2} \right) O_2 = \bar{I}t - O_1 t + T_s \cdot O_1 + \frac{t}{2} O_1 = (\bar{I} - O_1)t + \left(T_s + \frac{t}{2} \right) O_1$$

$$O_2 = (\bar{I} - O_1) \frac{t}{\left(T_s + \frac{t}{2} \right)} + O_1, \quad C = \frac{t}{\left(T_s + \frac{t}{2} \right)}$$

$$O_2 = (\bar{I} - O_1)C + O_1 \quad (14)$$

C is a proportioning time constant, where t is the daily time step (24 hours) and T_s is time of storage also in hours. Equation (16) is the numerical iterative core of the algorithm in the method of cascading weirs. USACE SSARR manual refers to this routing technique as the *Method of Cascading Weirs*. Figure 11 shows the series of weirs and the use of routing equation (14). The weirs or phases (a and b) are series of linear storage. The output for the current time period applies equation (14), which will be used to solve the mean input into the next phase. The last phase, b , for example, uses the current output solution of phase b as the flow rate at the endpoint of the reach. USACE [32, 33] illustrates this method also as a series of buckets or containers with a hole at the bottom, pouring into one, and one to the next, and so on. Increasing the number of weirs or phases increases lag and attenuation in the hydrograph while time in storage value controls the attenuation or pulse input distribution over time.

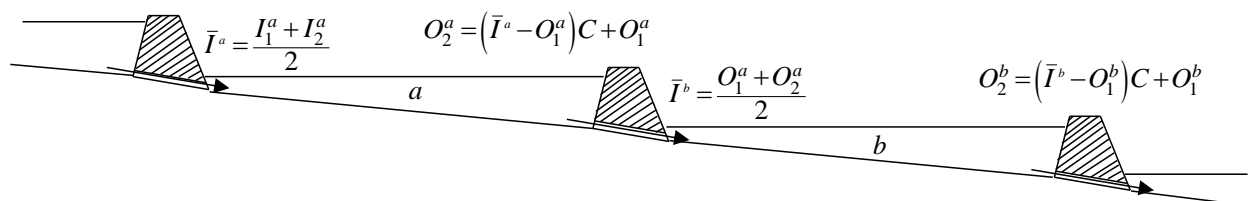


Figure 11. Depiction of the Method of Cascading Weirs.

In VADOCHARGE, the same idea of cascading weirs is used, vertically oriented as a series of phase cells (Figure 12). The conceptual model in Figure 7 depicts this series as a vertically arranged set of hour glass bulbs.

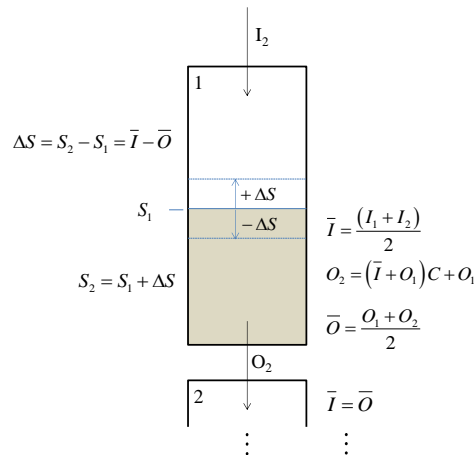


Figure 12. Routing applied in a phase cell series. Similar to the method of cascading weirs (Figure 11), this is the depiction of phase cell percolation, in vertical arrangement of a set of imaginary containments beneath its node-shed soils to the water table reach.

3.3 Computer Algorithm

The VADOCHARGE computer model is described here as flow diagrams for each of the two component modules: soil moisture and routing. The implementing code is built in *Microsoft® Visual Basic 6.0 Professional*, and is available in the appendix section in Habana et al. [12], web link provided.

3.3.1. Soil Moisture Algorithm

The soil moisture concept to algorithm assumes the soil absorbs all of its moisture from rainfall, no surface runoff. If the moisture input causes the soil moisture to exceed the field capacity, then the excess moisture is assigned to recharge. Then, the pan evaporation will further reduce the soil moisture depending on remaining soil moisture. If pan evaporation exceeds field capacity, soil moisture is reduced to zero (Figure 13).

The node-shed recharge is stored in an array variable, for each day and zone in the domain, and the area-weighted average recharge for each node-shed and day is computed at each time step by summing the product of each area's recharge times its area and then dividing this sum by the node-shed area. Area weighted summaries for the entire domain are computed by area weighted averages of the zones in the node-shed, and weighted average of node-sheds to the domain.

VADOCHARGE maintains a detailed record of the soil moisture variables for verification and summaries. Calculations for daily time steps can be used to calculate and display monthly and annual statistics for rainfall, pan evaporation, evapotranspiration, changes in soil moisture, and pan coefficients - as the ratio of modeled evapotranspiration to pan evaporation (potential evaporation). The summary output is displayed in a tab and can be saved as an Excel output file. This allows the modeler to examine the monthly and yearly averages when sampling different soil properties curve model settings. The array variable moisture to recharge, for each node-shed in the domain and day, is then used in the next algorithm module, Routing, that process the effect of fast and slow flow rates of lagged and attenuated recharge that reach and feed into the phreatic model surface node-cells.

3.3.2 Routing Algorithm

The SSARR routing technique described above is implemented in a second module to simulate the delay and attenuation of recharge through the thick karst to the water table, along each of the two alternative routes: slow and fast (Figure 14). The node-shed recharge is split by percent of recharge to fast flow and the remainder to slow flow. Each respective rate flow applies the router function. To the right of the figure is the router function general core algorithm code as depicted in Figure 12. NPS is the number of cell phases, MI is the mean input, and the PH phase array serves as a storage variable of previous period output for the phase cell and its node-shed. First, the area weighted average recharge for a node-shed is split by the fast/slow recharge split curve. The resulting fraction that goes into fast flow recharge is dependent on the bedrock moisture capacity, and the remaining moisture goes into the slow flow router. The router itself is a function algorithm that applies a visual basic *for loop* to the node-shed fast or

slow cascading phase cell series. The function variables are time in storage, number of phases, node-shed recharge, and a phase array. Below is the general program flow diagram for the router module.

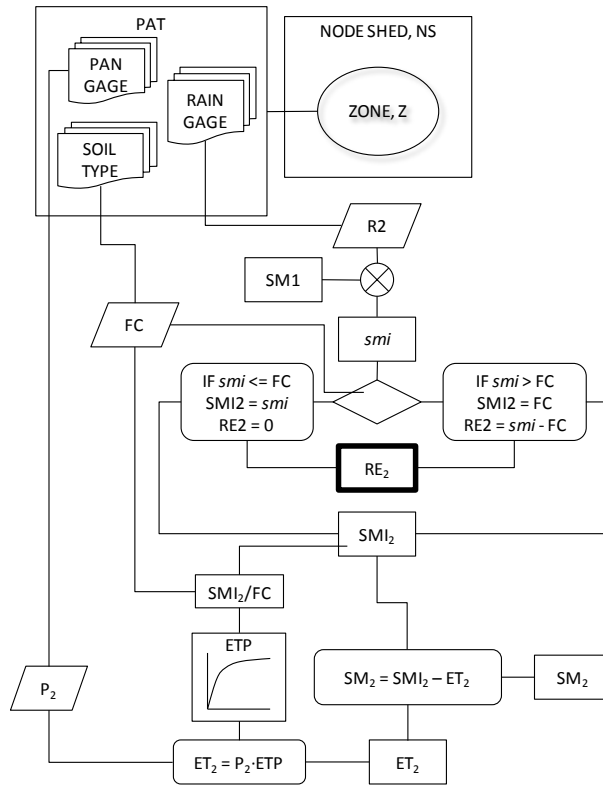


Figure 13. Zone recharge and node-shed recharge algorithm of soil moisture model. The algorithm goes through all the zones in the domain in reference to the polygon attribute table (PAT). The collection of daily computation of zonal moisture to recharge is used to determine each of the optional daily node-shed area weighted average moisture to recharge or node-shed sum of zonal moisture to recharge.

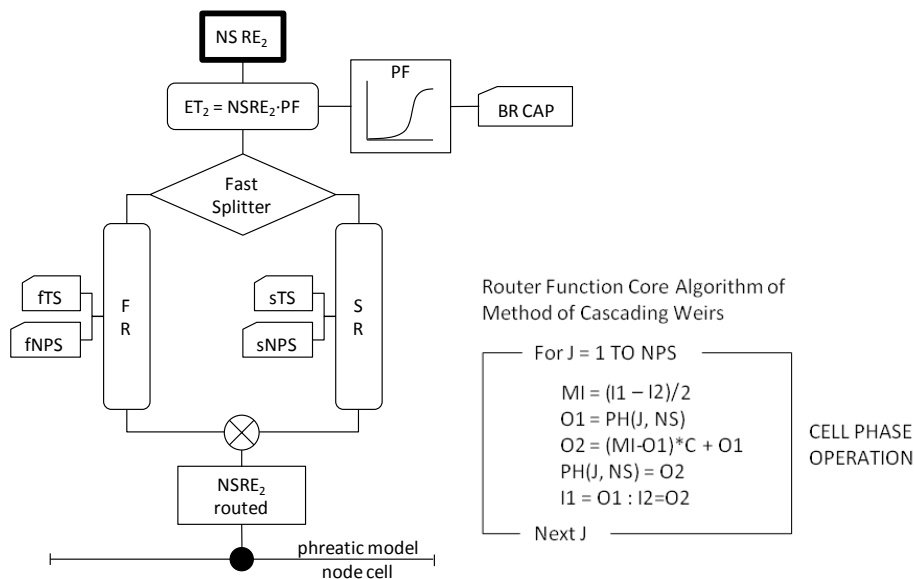


Figure 14. The general programming configuration of the router model.

3.4. Data Assembly

The recharge model node-shed (Figures 6 and 7) are constructed and fixed upon the node cells of the plan-view mesh of the underlying phreatic model (Figure 4). The spatial data is prepared first by constructing a phreatic finite element mesh, in this case 2-D quad-linear. VADOCHARGE was intended to provide meteoric recharge on node-cell phreatic surfaces, as gravitational driven flux through porous media, thus may apply to other phreatic mesh configurations with respect to the intentions.

Spatial data is prepared via ESRI™ ArcMap, Geographic Information System (GIS). A GIS technique *Euclidean Allocation* is used to create the node-sheds to the groundwater model mesh nodes. Next, is the superimposition of the soils layer polygons and the rainfall and pan evaporation Euclidean allocation (Theissen Polygons) layers. A GIS tool called Union combines all the layers to create a unique polygon attribute table (PAT) layer, which each polygon contains all the attributes for the polygons in each node-shed. Each entry in the table identifies the polygon references, soil type, rain gage, pan evaporation, and areas associated with the node-shed. The PAT is linked to input data spreadsheets containing the associated values for precipitation, pan evaporation, and soil properties.

The temporal data are rain and pan evaporation data [28] of daily records from 1982 to 1995. Two rain gages, Dededo and WSMO (Weather Service Meteorological Observatory, and two pan evaporation stations, NAS (Naval Air Station) and WSMO, are regionally separated by Theissen polygons. The boundary lines (gray straight lines) are seen going across the domain in Figure 5.

3.5. User Interface

VADOCHARGE is built with an interactive user interface (Figure 15) to facilitate configuration and running of the vadose model, which runs in conjunction with a coupled phreatic model¹. Configuration of the vadose model begins with loading the data: rainfall, pan evaporation, soil parameters, and PAT. After the data are loaded, the interface first takes the user through the soil moisture module. The output from this module includes a verification tab to check the computations. A summary tab displays the monthly and annual overall area-weighted averages. Next, a routing tab is enabled so that user can initiate the routing portion of the program. The final tab of this module includes a button that opens the underlying phreatic model's interface form.

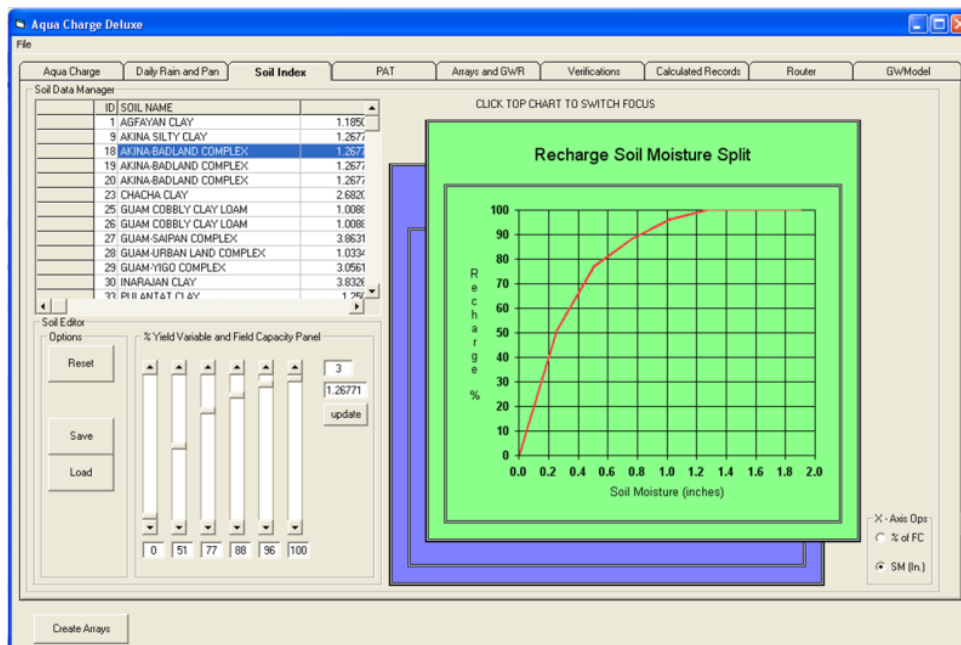


Figure 15. User interface for setting the soils properties curve, the Soil Index tab. The soil moisture curve is shown for recharge curved relationship.

¹ To support the development of the vadose model, the authors prepared a simple phreatic model, as the platform to support development of the vadose model, VADOCHARGE results may be used as input to any phreatic model.

4. RESULTS AND DISCUSSION

To evaluate the skill of the model, a history-matching exercise was done to compare the model's predictions against observed responses of the water table in selected observation wells. The exercise used the existing soils data for northern Guam [34] and the hydrologic data set from 1982 through 1995 [28]. The coupled model was run at daily time steps. Note that the phreatic platform used for the initial development of VADOCHARGE is a simple groundwater flow model that does not include the two-phase dynamics of a floating freshwater lens. (Using a more sophisticated phreatic model would have required excessive investment in the development and configuration of the phreatic model at the expense of resources for the development of the vadose model). More accurate and precise testing of the response of the water table (and saltwater interface) to changes in recharge eventually requires coupling the model to a two-phase, freshwater-seawater phreatic model (e.g., USGS SUTRA, for example). The results of our initial test are sufficiently accurate which was compared with historic data to determine the vadose model performance is correct and realistic.

4.1 Soil Model Conditions

Three soil moisture ET curve conditions were applied and analyzed for the thin soil layers on the domain. Soil model 1 applies Thornthwaite ET curve, model 2 is Viemeyer, and model 3 is Pierce. Figure 16 shows monthly and yearly averages for the models labeled M1 to M3, with respect to the soil model curves used; and ET and GWR is evapotranspiration and moisture to recharge (not routed). M1, Thornthwaite model, most nearly agrees with Mink's "most probable" estimate [23] of 65% of annual rainfall (approximately 2540 mm) goes to recharge. Figure 17 are soil model average by month. Figure 18 shows a sample of the daily routed recharge synthesis results between the ET models used.

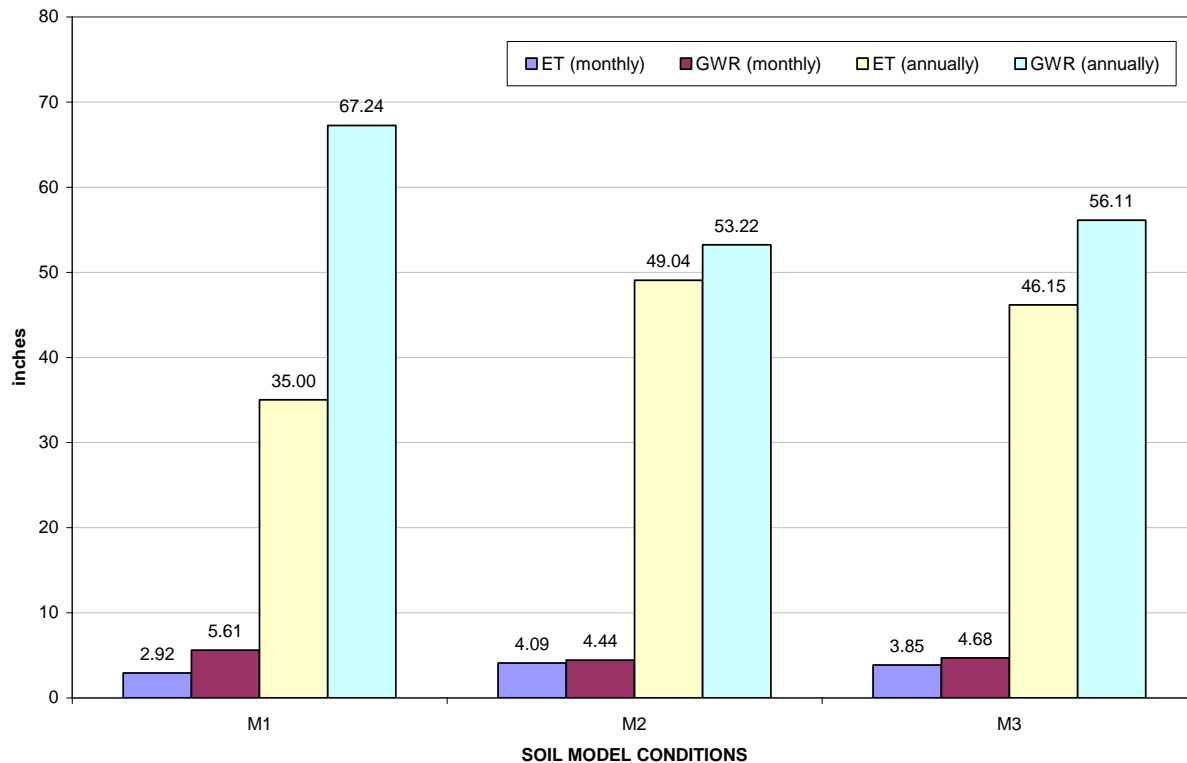


Figure 16. Soil moisture model results for 3 different soil moisture curve scenarios.

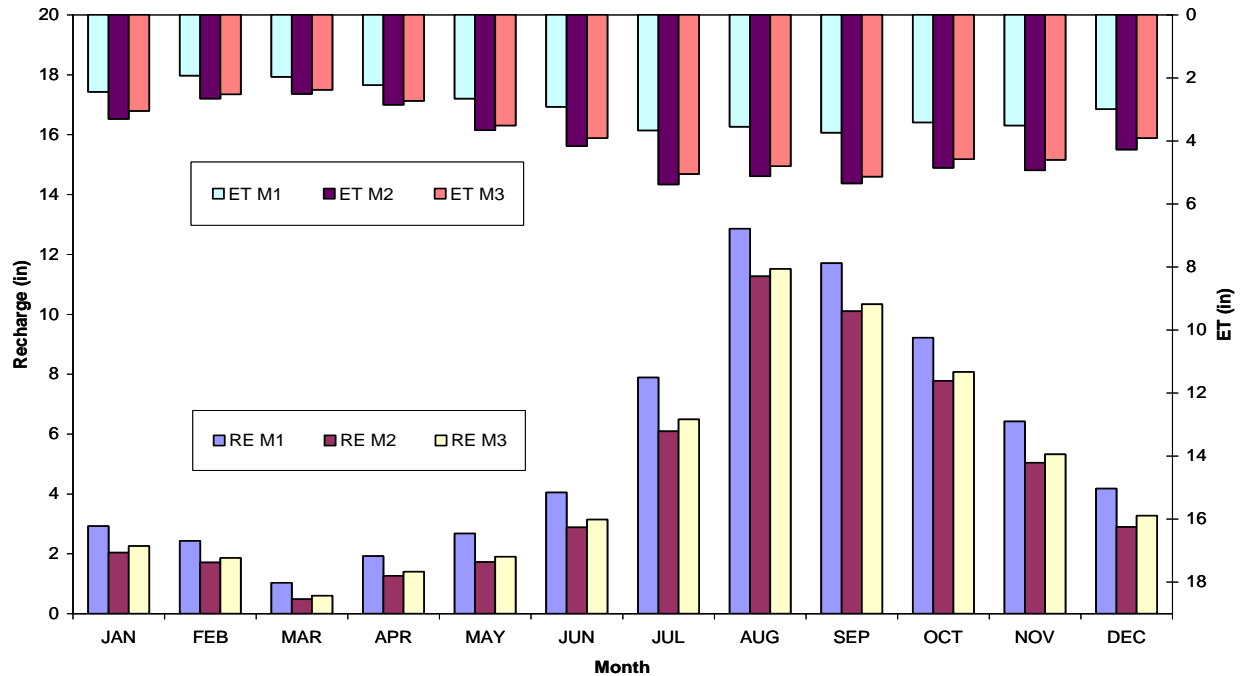


Figure 17. Monthly model comparison bar chart. Soil Model comparison chart shows ET values (top secondary axis) and Recharge (primary axis) for the three models. RE is moisture to recharge.

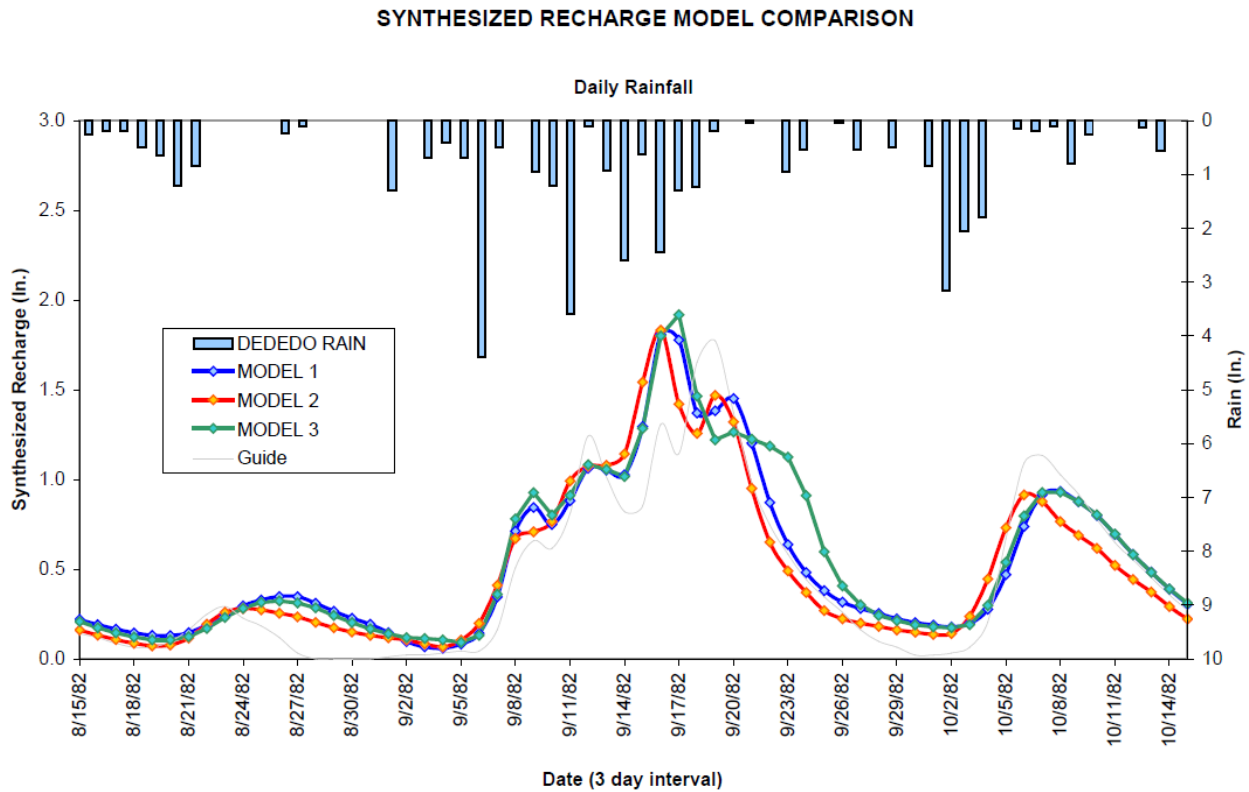


Figure 18. Recharge synthesis test results of three different ET curve models. This was done maintaining a set time of storage and phase of the router for each soil curve model to show the difference between each.

4.2. Summaries

For the selected model, the area-weighted average (Stage 1) summaries were calculated for the domain. Table 1 is the summary for the application of the Thornthwaite ET model.

MONTH	RAIN	PAN	ET	GWR	PAN COEF	DEL SM	YEARS	RAIN	PAN	ET	GWR	PAN COEF
JAN	131	155	62	74	0.40	-68	MONTHLY 1982-1995	216	167	74	142	0.44
FEB	112	154	49	62	0.32	15	YEARLY 1982-1995	2597	2004	889	1708	0.44
MAR	73	189	50	26	0.26	-41						
APR	107	202	57	49	0.28	20						
MAY	140	199	68	68	0.34	63						
JUN	178	179	74	103	0.41	20						
JUL	298	165	93	200	0.57	65						
AUG	416	147	90	327	0.61	-5						
SEP	392	152	95	297	0.62	-11						
OCT	321	141	87	234	0.61	10						
NOV	248	169	89	163	0.53	-53						
DEC	181	152	76	106	0.50	-16						

Table 1. Monthly and annual summaries. Soil moisture model computed averages (mm) for the entire domain, using Thornthwaite ET curves. GWR is moisture to recharge, PAN is pan evaporation, PAN COEF is pan coefficient as ratio of computed ET to PAN, and DEL SMI is change in soil moisture.

4.3. Recharge Simulation

A few samples are given (Figures 19 and 20) of recharge synthesis for the node-sheds at observation well sites M-11, and only a few because the charts extend daily from 1982 to 1995 with more than 130 node-sheds (more simulation samples in the technical report, Habana et al. [12]). The program design computes results in inches into the charts. The chart is made to scroll along the time domain and the visible window is set to about two months.

Figure 19 shows the results of recharge simulation at the node-shed fixed upon observation well M-11 (see Figures 4 and 5). The chart date spans from 8/6/1992 to 10/7/1992, when Typhoon Omar poured in more than 3800 mm of rain. That event caused a significant response in the water level at the observation site to more than 2 m. In the chart, the gray curve is an estimated porosity scaling of the observation record, the blue is fast flow, the green is slow flow, and the red is the sum of fast and slow flows. This point is influenced by the DED (Dededo) rain data. The gray line is an estimated pore scale of the observation data used to estimate the shape of the recharge hydrograph simulation that would cause the water levels to respond as such. M-11 observation well is a good place to make estimates for the hydrograph shapes because of its sharp response to rain events and slow recovery rate.

Figure 20 shows the rainy season recharge simulation between 9/14/1993 to 11/15/1993. In this recharge synthesis, two rain events a week apart of more than 75 mm of rain produces a double response of fast flow occurring before the peak of the long attenuated slow flow.

4.4. Recharge Synthesis and Groundwater Model Response

The following figures (21 and 22) are the results of a 2-D finite element, transient, saturated groundwater model, response to the synthesized recharge. Again, the results are matched to observation well data at M-11. For each figure, the top hydrograph is the recharge synthesis at the node-shed at M-11, and the bottom chart is the phreatic model simulation response to synthesized recharge. The phreatic model parameters, hydraulic conductivity used were between 1500-6000 m/d and specific storage between 0.00005-0.0003 m^{-1} . Small specific storage provided amplitude to hydraulic head. To achieve a flashy response as in M-11 required the lower hydraulic conductivities and specific storage. Less than 800 m/d hydraulic conductivity resulted erratic oscillation. The less responsive M-10a observation data required higher specific storage of up to 0.01 m^{-1} .

4.5. Discussion

The development of VADOCHARGE required a thorough understanding of the study area's hydrology, geology, and hydrogeology, of uplifted carbonate island karst aquifer system. Water level response to rainfall revealed a striking similarity to hydrographs of surface hydrology, which led to the idea of applying surface hydrologic methods as an analogue model. The VADOCHARGE model allowed the daily transient modeling of attenuated and lagged flows through the aquifer at each node-shed, that when coupled to the phreatic model, improved simulation and history match, while all former phreatic models operated in monthly time steps and steady state. Refined estimates of recharge improves estimate of the water source budget, which can suggest water source limitations through seasonal weather.

The model could be improved and further developed. Landcover maps can provide improved surface details, such as accounting for intercept over impervious surfaces and vegetation, thus refining moisture input. The establishment of this code allows the model development into other application platforms, programming into GIS or Microsoft® Excel (which is now being done). The rapid change of program versions or operating systems make the software short lived, thus the need to seek time tested applications. In process, the VADOCHARGE is undergoing new development to include solute transport, specifically the modeling of N from domestic wastewater discharge into the NGLA.

In this experience, as common to many groundwater modeling endeavors, the greatest limitation is available data [19]. Currently, there is much data, but spatially far apart, leaving the modeler to wide or regional coverage. Increased rain and pan gages would localize the area of influence, making smaller areas of Theissen Polygons and improve rainfall input and ET quantification. Another issue, although the VADOCHARGE is designed and programmed to accommodate spatial variation to every node-shed in the domain, the parameter settings are limited to the available observation wells. One can only assume that the time and phase parameters for the other node-sheds are not so much different, but unfortunately it remains uncertain and not something to feel so confident that it is when dealing with karst. The need for more observation wells or monitoring data is essential to any model's quest for accuracy and would improve model calibration, sensitivity testing, and confidence in interpretation of model results. The problem of installation of observation well at strategic locations is cost and property issues. Drilling 60-180 m deep to the phreatic zone is not a cheap operation in Guam (can range from 50-100 thousand dollars), and obtaining permission to do so at desired locations is not as easy as it sounds. However, with a model built and civil development increasing, concerned agencies in Guam may find the importance, if management is in pursuit of accuracy to make decisions.

VADOCHARGE is now an antecedent model for a solute transport model for Guam, undergoing modifications to include the simultaneous simulation of the nitrogen (N) cycle transport from domestic discharge. This new model has added an interception process, wastewater N fate and transport, and is now programmed in Microsoft's® Excel's Visual Basic Editor Platform, called VADOCHARGE-N. The new platform allows the model to be easily modified and upgraded in the developer and may easily transfer and survive the rapidly changing and upgrading current technology.

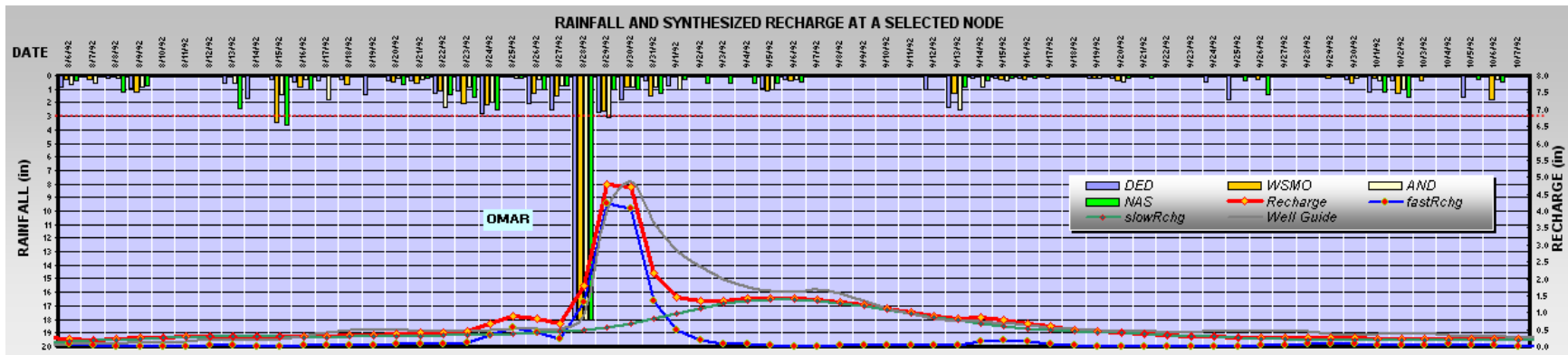


Figure 19. Recharge simulation of Typhoon Omar, late August 1992, which poured more than 380 mm (15 in) of rain.

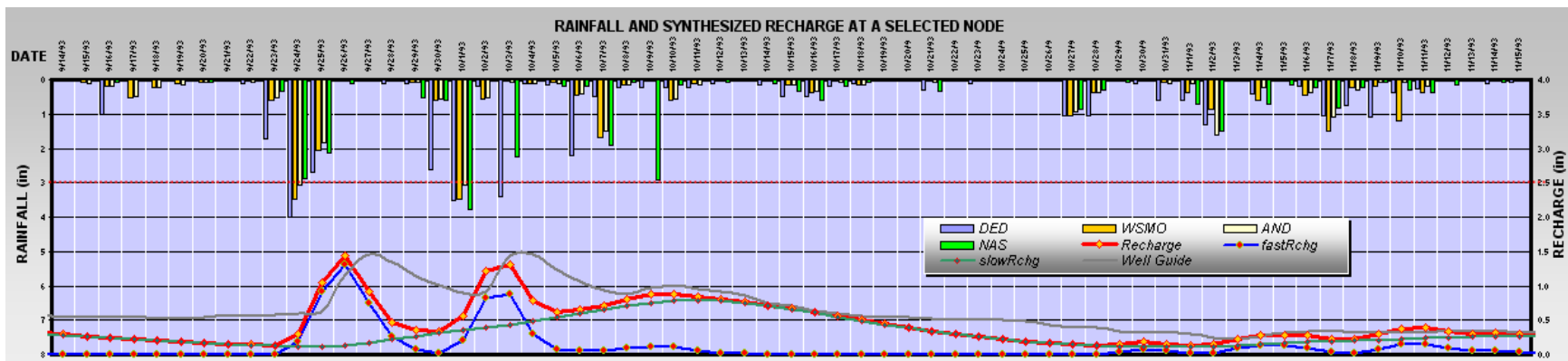


Figure 20. Recharge simulation of two rain input pulses a week apart. Recharge hydrograph shows two rapid responses with the long attenuated slow flow for the rain events.

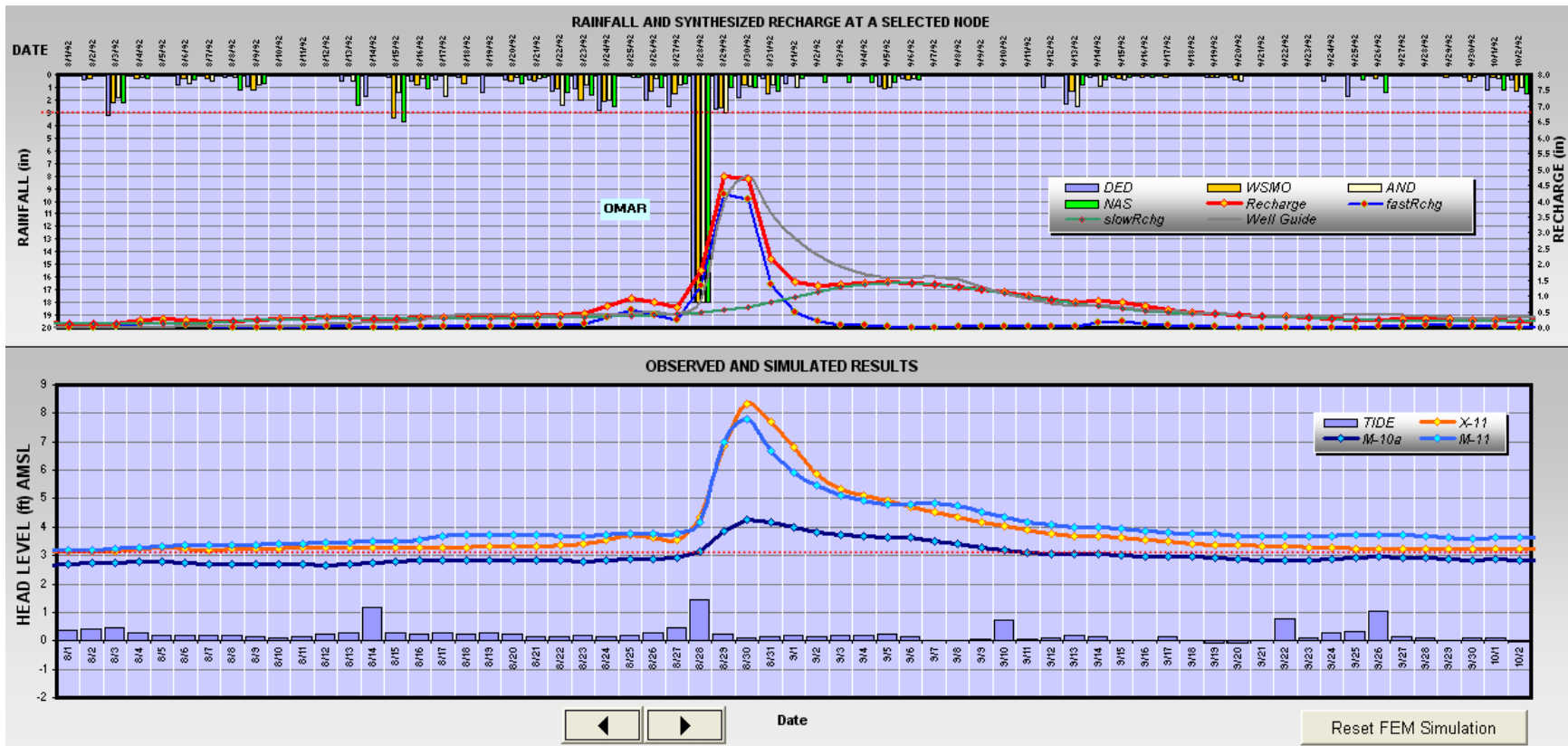


Figure 21. Typhoon Omar, August 28, 1992. The significant amount of rain for this event really captures the similarity of groundwater response to that of streamflow hydrographs. The lower chart, the simulation is the orange curve (labeled X-11 in the legend), the observed water level at M-11 is light blue, and the observed water level at M-10a is dark blue.

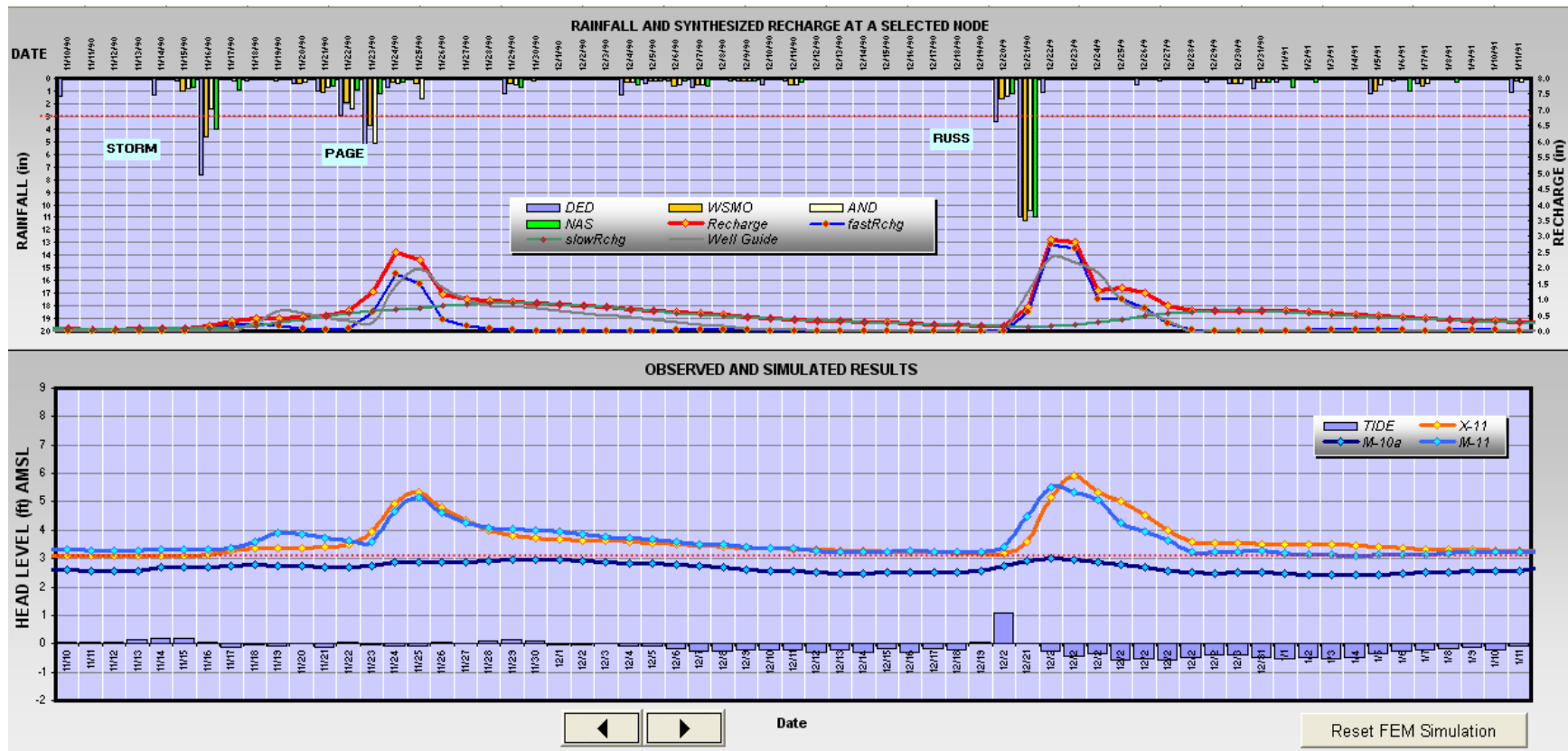


Figure 22. Three storms near the end of 1990. Storm page rain values form a wide fast flow (blue – top chart) and the slow flow from the two storms produce wide attenuations. The groundwater simulation response (orange) nearly matches observation well data (light blue) from the recharge synthesis of storm page. Storm Russ produces an unusual shape of synthesized fast recharge.

5. CONCLUSION

VADOCHARGE provides a simple, efficient, and improved model of vadose transport through the vadose zone of a karst aquifer, especially for thick vadose zones in which there are substantial differences between the rates of percolation through the matrix and rapid descent through fast flow routes. It includes the necessary soil attributes and hydrologic data, and organizes the domain in an easily understandable configuration. The soil moisture model improves the evapotranspiration estimates, thus improving recharge estimates past the soil. The router provides a quick and efficient computing tool for producing realistic simulations of the recharge flux to the water table along the separate flow paths. The synthesis focuses on the time arrival of recharge to the water-table rather than the path through the complex hydrogeology of the limestone media. The model allowed the shaping of recharge curves that would probably cause such observation well responses seen in the hydrographs.

REFERENCE

- [1] Atkinson TC (1977). Diffuse flow and conduit flow in limestone terrain in the Mendip Hills Somerset (Great Britain). *J. Hydrol.* 35:93-110.
- [2] Ayers JF (1981). Estimate of recharge to the freshwater lens of Northern Guam. Water Resource Research Center (WRRC², now WERI) of the Western Pacific, University of Guam (UOG). Technical Report (TR) 21.
- [3] Ayers JF, Clayshulte RN (1984). A Preliminary Study of the Hydrogeology of Northern Guam. WERI, UOG TR 56.
- [4] Bear J, Beljin MS, Ross RR (1992). Fundamentals of Ground-Water Modeling. US EPA Ground Water Issue 540/S-92/005:1-11.
- [5] Camp Dresser and McKee (CDM), Inc., in association with Barrett, Harris and Associates (BHA), Inc. (1982). Final Report, Northern Guam Lens Study, Groundwater Management Program. Aquifer Yield Report for Guam Environmental Protection Agency.
- [6] Contractor DN (1981). A Two-dimensional, Finite-element Model of Salt Water Intrusion in Groundwater Systems. WERI, UOG, TR 26.
- [7] Contractor DN, Srivastava R (1989). Calibration of a Saltwater Intrusion Model for the Northern Guam Lens Using a Microcomputer. WERI, UOG, TR 69.
- [8] Contractor DN, Jenson JW (1999). Simulated Effect of Vadose Infiltration on Water Levels in the Northern Guam Lens Aquifer. WERI, UOG, TR 90.
- [9] Ford DC, Williams P (2007). Karst Hydrogeology and Geomorphology. John Wiley & Sons Ltd, England.
- [10] Fox IA, Rushton KR (1976). Rapid recharge in a Limestone Aquifer. *Groundwater* 14:21-27.
- [11] Fread DL (1985). Hydrological Forecasting: Chapter 14 Channel routing. John Wiley and Sons Ltd., p 437-501.
- [12] Habana NC, Heitz LF, Olsen AE, Jenson JW (2009). Vadose Flow Synthesis for the Northern Guam Lens Aquifer. WERI, UOG, TR 127, www.weriguam.org³.
- [13] Heitz LF (2006). Personal communications. Emeritus Professor of Hydrology, WERI, UOG.
- [14] Hillel D (1977). Computer Simulation of Soil-Water Dynamics, A Compendium of Recent Work. International Development Research Centre, Canada.
- [15] Hoffman MS, Jenson JW, Denton GRW (2007). Background Fluorescence in Guam's Coastal Groundwater. WERI, UOG, TR 121.
- [16] Jenson JW, Keel TM, Mylroie JR, Mylroie JE, Stafford KW, Taborosi D, Wexel C (2006). Karst of the Mariana Islands: The Interaction of Tectonics, Glacio-Eustasy, Fresh-Water/Salt-Water Mixing in Island Carbonates. Geological Society of America, Special Paper, 404:129-138.
- [17] Jocson JMU (1998). Hydrologic Model for the Yigo-Tumon and Finegayan Sub-basins of the Northern Guam Lens Aquifer. WERI, UOG Master's Thesis.
- [18] Jocson JMU, Jenson JW, Contractor DN (2002). Recharge and aquifer response: Northern Guam Lens Aquifer, Guam, Mariana Island. *Journal of Hydrology* 260:231-254.
- [19] Konikow LF, Bredehoeft JD (1992). Ground-water models cannot be validated. *Advances in Water Resources* 15:75-83.

² Former names: Water Resource Research Center(1977-1980), Water and Energy Research Institute of the Western Pacific (1976, 1981-1998), Water and Environmental Research Institute of the Western Pacific (1998-present).

³ All WERI, UOG Technical Reports in reference are available at this site.

- [20] Lander MA (1994). Meteorological factors associated with drought on Guam. WERI, UOG, TR 75.
- [21] Lander MA (2001). Responses of well water levels on Northern Guam to variations of rainfall and sea level. WERI, UOG, TR 94.
- [22] Mink JF, Branch JB, Worlund J, BHA, CDM (1982). Summary Report Northern Guam Lens Study. Guam EPA.
- [23] Mink JF (1991). Groundwater in Northern Guam: Sustainable Yield and Groundwater Development. Barrett Consulting Group for Public Utility Agency of Guam.
- [24] Moran DC, Jenson JW (2004). Dye Trace of Groundwater Flow from Guam International Airport and Harmon Sink to Agana Bay and Tumon Bay, Guam. WERI, UOG, TR 97.
- [25] Mylroie JE, Jenson JW (2000). The Carbonate Island Karst Model Applied to Guam. Theoretical and Applied Karstology 13(14):51-56.
- [26] Rotzoll K, Gingerich SB, Jenson JW, el-Kadi AI (2013). Estimating hydraulic properties from tidal attenuation in the Northern Guam Lens Aquifer, territory of Guam, USA, Hydrogeology Journal. ##:##-##.
- [27] Rushton KR, Ward C (1979). The estimation of groundwater recharge. Journal of Hydrology 41:345-361.
- [28] National Climatic Data Center (NCDC) (2011). Climatedata and Hydrodata. Hydrosphere, annual compact disc subscription.
- [29] Stearns HT (1937). Geology and water resources of the island of Guam, Mariana Islands. US Navy Manuscript Report.
- [30] Tracey JJ, Schlanger SO, Stark JT, Doan DB, May HG (1964). General Geology of Guam, Mariana Islands. US Geologic Survey Professional Paper.
- [31] US Army Corps of Engineers (USACE) North Pacific Division (NPD) (1987). User Manual, Microcomputer Version of the Streamflow Synthesis and Reservoir Regulation (SSARR) Model (draft as of 1987). USACE, NPD, Portland, Oregon.
- [32] USACE (1990). River routing with HEC-1 and HEC-2. USACE Hydrologic Engineering Center, Training Document 30.
- [33] USACE (1994). Engineering and Design, Flood-Runoff Analysis. USACE Engineer Manual 1110-2-1417:1-214.
- [34] U.S. Department of Agriculture (USDA), Natural Resource Conservation Service (NRCS) (1988). Soil Survey of the Territory of Guam. National Cooperative Soil Survey, USDA, NRCS (SCS), UOG, and Department of Commerce, Guam.
- [35] Vacher HL, Mylroie JE (2002). Eogenetic karst from the perspective of an equivalent porous medium. Carbonates and Evaporites 17:182-196.
- [36] van Genuchten MT, Nielsen DR (1985). On Describing and Predicting the Hydraulic Properties of Unsaturated Soils. Ann. Geophys. 3:615-628.
- [37] Voss CI, Provost AM (2010). SUTRA, A Model for Saturated-Unsaturated Variable Density Groundwater Flow with Solute or Energy Transport. Water Resources Investigation Report 02-4231, Reston, Virginia.
- [38] Vann D et al. (2002, 2013). Updated GIS Shapefile of the Basement Volcanic Contour Map of the Northern Guam. Unpublished, WERI, UOG.
- [39] Ward AD, Trimble SW (2004). Environmental Hydrology, 2nd Edition. CRC Press LLC, Lewis Publishers.
- [40] Ward PE, Hafford SH, Davis DA (1965). Hydrology of Guam, Mariana Islands. USGS Professional Paper 403-H:25 pp.
- [41] Worthington SRH (2003). A comprehensive strategy for understanding flow in carbonate aquifer. Speleogenesis and Evolution of Karst Aquifers 1(1):1-8.